# Synaptic fatigue at the naive perforant path–dentate granule cell synapse in the rat

Therése Abrahamsson, Bengt Gustafsson and Eric Hanse

*Department of Physiology, Institute of Physiology and Pharmacology, Göteborg University, Göteborg, Sweden*

**Synaptic activation at low frequency is often used to probe synaptic function and synaptic plasticity, but little is known about how such low-frequency activation itself affects synaptic transmission. In the present study, we have examined how the perforant path–dentate granule cell (PP–GC) synapse adapts to low-frequency activation from a previously non-activated (naive) state. Stimulation at 0.2 Hz in acute slices from developing rats (7–12 days old) caused a gradual depression of the AMPA EPSC (at −80 mV) to about half within 50 stimuli. This synaptic fatigue was unaffected by the NMDA and metabotropic glutamate (mGlu) receptor antagonists D-AP5 and LY-341495. A smaller component of this synaptic fatigue was readily reversible when switching to very low-frequency stimulation (0.033–0.017 Hz) and is attributed to a reversible decrease in release probability, which is probably due to depletion of readily releasable vesicles. Thus, it was expressed to the same extent by AMPA and NMDA EPSCs, and was associated with a decrease in quantal content (measured as $1/CV^2$) with no change in the paired-pulse ratio. The larger component of the synaptic fatigue was not readily reversible, was selective for AMPA EPSCs and was associated with a decrease in $1/CV^2$, thus probably representing silencing of AMPA signalling in a subset of synapses. In adult rats (> 30 days old), the AMPA silencing had disappeared while the low-frequency depression remained unaltered. The present study has thus identified two forms of synaptic plasticity that contribute to fatigue of synaptic transmission at low frequencies at the developing PP–GC synapse; AMPA silencing and a low-frequency depression of release probability.**

(Resubmitted 29 August 2005; accepted after revision 17 October 2005; first published online 20 October 2005)
**Corresponding author** T. Abrahamsson: Göteborg University, Department of Physiology, Box 432, Medicinaregatan 11, 405 30 Göteborg, Sweden. Email: therese.abrahamsson@physiol.gu.se

Activity-dependent alterations in synaptic efficacy, synaptic plasticity, is generally seen as a phenomenon arising as a consequence of repetitive synaptic activation in the higher frequency range ($\geq$ 1 Hz). However, even activation at intervals of tens of seconds can result in depression of synaptic efficacy (Castellucci & Kandel, 1974; Teyler & Alger, 1976; White *et al.* 1979; Xiao *et al.* 2004). Such synaptic fatigue has been linked to behavioural habituation (Christoffersen, 1997). For example, short-term habituation of the gill withdrawal reflex in *Aplysia* is caused by homosynaptic depression at the sensorimotor neurone synapses (Castellucci & Kandel, 1974). A total silencing of a subset of synapses has been proposed as the most likely mechanism underlying this homosynaptic depression (Gover *et al.* 2002). In the dentate gyrus of the hippocampus, the perforant path–granule cell (PP–GC) synapse in the adult rat exhibits synaptic fatigue induced by stimulation in the low-frequency range (0.05–0.2 Hz), referred to as habituation (Teyler & Alger, 1976; White *et al.* 1979). What underlies this form of synaptic fatigue is yet unexplored.

Hippocampal CA3–CA1 synapses in the developing, but not in the adult animal (> 30 days old), exhibit synaptic fatigue in response to synaptic activation in the low-frequency range (0.05–0.2 Hz) (Xiao *et al.* 2004). This synaptic fatigue has been explained by total AMPA silencing in a subset of the synapses. In contrast to CA1 pyramidal neurones, dentate granule cells are generated postnatally and new granule cells are continuously generated throughout adulthood, albeit at a low rate (Altman & Das, 1965; Schlessinger *et al.* 1975). The constant renewal of granule cells raises the possibility that forms of synaptic plasticity that are otherwise restricted to the developmental period, such as AMPA silencing, are maintained in the adult animal, and may underlie synaptic fatigue of these synapses.

In the present study we have examined synaptic fatigue at PP–GC synapses of developing and adult rats. We found

 DOI: 10.1113/jphysiol.2005.097725

that these synapses exhibit pronounced synaptic fatigue, albeit to a larger extent in the developing animals. This fatigue could be partly explained by AMPA silencing; however, only in the developing animals. In the adult rats, and to an extent in the developing animals, the synaptic fatigue was explained by depression of presynaptic release probability most probably related to depletion of readily releasable vesicles.

## Methods

### Slice preparation and solutions

Experiments were performed on hippocampal slices from 7- to 47-day-old Wistar rats. Most of the experiments were performed on either 7- to 12-day-old rats (referred to as 'developing') or 30- to 47-day-old rats (referred to as 'adult'). The animals were killed in accordance with the guidelines of the Göteborg ethical committee for animal research. Rats older than 10 days were anaesthetized with isoflurane (Abbott) prior to decapitation. The brain was removed and placed in an ice-cold solution containing (mM): choline chloride 140, KCl 2.5, $CaCl_2$ 0.5, $MgCl_2$ 7, $NaHCO_3$ 25, $NaH_2PO_4$ 1.25, ascorbic acid 1.3 and dextrose 7. Transverse hippocampal slices (thickness, 300–350 $\mu$m) were cut with a vibratome (Slicer HR 2, Sigmann Elektronik, Germany) in the same ice-cold solution and they were subsequently stored in artificial cerebrospinal fluid (ACSF) containing (mM): NaCl 124, KCl 3, $CaCl_2$ 2, $MgCl_2$ 4, $NaHCO_3$ 26, $NaH_2PO_4$ 1.25, ascorbic acid 0.5, *myo*-inositol 3, D,L-lactic acid 4 and D-glucose 10 at 25°C. After 1–8 h of storage, a single slice was transferred to a recording chamber where it was kept submerged in perfusion ACSF at a constant flow (~2 ml $min^{-1}$) at 30–32°C. The perfusion ACSF contained (mM): NaCl 124, KCl 3, $CaCl_2$ 4, $MgCl_2$ 4, $NaHCO_3$ 26, $NaH_2PO_4$ 1.25 and D-glucose 10. Picrotoxin (100 $\mu$M) was always present in the perfusion ACSF to block $GABA_A$ receptor-mediated activity. All solutions were continuously bubbled with 95% $O_2$ and 5% $CO_2$ (pH ~7.4). The higher than normal $Ca^{2+}$ and $Mg^{2+}$ concentrations were used to block spontaneous network activity.

### Recording and analysis

Electrical stimulation of perforant path afferents was carried out in the outer two-thirds of the molecular layer. Stimuli consisted of biphasic constant current pulses (200 + 200 $\mu$s, 5–40 $\mu$A, STG 1004, Multi Channel Systems MCS Gmbh, Reutlingen, Germany) delivered through a glass pipette (resistance ~0.5–1 MΩ). Whole-cell patch-clamp recordings were performed on visually identified dentate granule cells, using infrared–differential interference contrast videomicroscopy mounted on a Nikon E600FN microscope (Nikon, Japan). The pipette solution contained (mM): caesium methanesulphonate 130, NaCl 2, Hepes 10, EGTA 0.6, QX-314 5, Mg-ATP 4 and GTP 0.4, or caesium methanesulphonate 110, NaCl 2, Hepes 10, BAPTA 10, QX-314 5, Mg-ATP 4 and GTP 0.4 (pH ~7.3; osmolality, 270–300 mosmol $l^{-1}$). The latter pipette solution was used to prevent possible long-term synaptic plasticity when train stimulation was used as the test stimulus (see Fig. 9). Liquid junction potential was both measured and calculated to be about 8 mV and it was not corrected for. Patch pipette resistances were 2–6 MΩ. EPSCs were recorded at a sampling frequency of 10 kHz and filtered at 1 kHz, using an EPC-9 amplifier (HEKA Elektronik, Lambrecht, Germany). Cells were held in voltage-clamp mode at −80 mV for AMPA EPSC recordings and +40 mV for NMDA EPSC recordings. Series resistance was monitored using a 5-ms, 10-mV hyperpolarizing pulse. Series resistance was not allowed to change more than 15%, otherwise the recording was not included in the analysis. EPSCs were analysed off-line using custom-made IGOR Pro (WaveMetrics, Lake Oswego, OR, USA) software. AMPA EPSCs were measured as the difference between the baseline level immediately preceding the stimulation artefact, and the mean amplitude during a 2-ms time window around the negative peak between 3 and 8 ms after the stimulation artefact. NMDA EPSCs were measured as the difference between the baseline level immediately preceding the stimulation artefact, and the mean amplitude during a fixed time window 14–19 ms after the stimulation artefact. During this time window, the AMPA EPSC contributes by less than 10% to the total amplitude as shown by the application of the AMPA receptor antagonist NBQX ($n = 3$). EPSC variability (CV) was estimated as S.D./mean. $1/CV^2$ values were calculated from 20 to 50 consecutive EPSCs, except for 0.033-Hz stimulation where 10 consecutive EPSCs were used. As the paired-pulse ratio did not change during synaptic fatigue or low-frequency depression (see Results), both EPSCs were used to calculate the change in $1/CV^2$ value to obtain a more accurate estimation in experiments using paired-pulse stimulation. Field EPSP recordings were made by means of a glass micropipette (filled with perfusion ACSF) in the molecular layer. Field EPSP magnitude was estimated by linear regression over the first 0.5–0.8 ms of the initial slope. The presynaptic volley was measured as the peak-to-peak amplitude of the initial positive–negative deflection. Data are expressed as means ± S.E.M. Statistical significance for paired and independent samples was evaluated using Student's *t* test.

### Drugs

Chemicals were from Sigma-Aldrich (Stockholm, Sweden) except for D-AP5, LY-341495, NBQX (Tocris Cookson, Bristol, UK) and QX-314 (Tocris Cookson, Bristol, UK and Alomone Laboratories, Jerusalem, Israel).

## Results

### Fatigue of AMPA EPSCs at naive synaptic inputs in the developing rat

To examine whether synaptic transmission is altered by the initiation of low-frequency activation, previously unstimulated (naive) PP–GC synapses were used. It was therefore not possible to adjust the position of the stimulus electrode or the stimulus intensity to obtain EPSCs of a certain magnitude. Instead we used a preselected stimulation intensity (5–40 $\mu$A, dependent mainly on animal age and cell capacitance), which in different experiments resulted in variable EPSC magnitudes (up to 1 nA). The magnitude of the very first evoked EPSC in each experiment was used as a reference for the naive synaptic strength, and the subsequently evoked responses were compared to this first reference EPSC.

As exemplified by Fig. 1*A*, activation of naive PP–GC synapses at 0.2 Hz in the developing rat (7–12 days old) led to a substantial depression of the AMPA EPSCs. The depression developed relatively quickly during the first 30–40 stimuli, after which the EPSC magnitude approached a relatively stable, albeit still slowly decaying, level. On average ($n = 7$), the AMPA EPSC was depressed to $45 \pm 6.0\%$ of its initial value within 40–60 stimuli (Fig. 1*B*). To evaluate possible changes in release probability in association with this synaptic fatigue, we subsequently used paired pulses (50 ms) at 0.2 Hz as a test stimulus (Fig. 1*C*). The paired-pulse stimuli resulted in a similar decay of the AMPA EPSC (to $55 \pm 3.2\%$ of its initial value within 40–60 stimuli, $n = 10$). Combining the results from both single and paired-pulse test stimuli ($n = 17$), the AMPA EPSC decayed to $51 \pm 3.2\%$ (of the naive AMPA EPSC amplitude) within 40–60 stimuli.

When evaluating possible changes in paired-pulse ratio from a group of experiments, there is a risk of obtaining false increases if individual ratios are averaged (Kim & Alger, 2001). To circumvent this problem, we constructed a ratio between the second and first EPSCs averaged over all the experiments using paired-pulse stimulation ($n = 10$). The time course of this ratio (Fig. 1*D*) shows that the AMPA EPSC fatigue develops without any associated change in the paired-pulse ratio.

To test whether the AMPA EPSC fatigue was related to NMDA and/or metabotropic glutamate (mGlu) receptor-dependent long-term depression (LTD), experiments were performed in the presence of D-AP5 (50 $\mu$M) and LY-341495 (20 $\mu$M). As shown in Fig. 1*E*, the AMPA EPSC fatigue developed similarly in the presence of these receptor antagonists, decaying to $55 \pm 2.9\%$ of the initial magnitude within 40–60 stimuli ($n = 16$).

We next examined whether the synaptic fatigue was based on a change in quantal size or quantal content using the $1/CV^2$ analysis (Clements, 1990; Korn & Faber, 1991). We thus estimated the EPSC variability ($1/CV^2$ value) in the early (the first 20 sweeps) and in the late (sweeps 40–60) phase of the fatigue. To obtain an estimate of the variance during these non-stationary (decaying) conditions, EPSC data were first fitted to an exponential function. Data were then divided (and thus normalized) by this exponential function and the variance was calculated, as illustrated for one experiment in Fig. 1*F*. Although there was some variation in the change of the $1/CV^2$ value between experiments (because of the necessity of using a restricted number of sweeps), the average decrease in $1/CV^2$ (to $74 \pm 9.7\%$, $n = 17$) matched quite well the corresponding decrease of the AMPA EPSC (to $68 \pm 2.7\%$, $n = 17$; note that the initial value here is based on the average of the first 20 EPSCs), indicating that the synaptic fatigue is caused by a decrease in quantal content.

### Two components of AMPA EPSC fatigue in the developing rat

To evaluate the reversibility of the AMPA EPSC fatigue, the stimulation frequency was lowered from 0.2 Hz to 0.033 Hz (a frequency at which fatigue should not be expected (White *et al.* 1979)) when a relatively stable level of synaptic fatigue had been obtained. This lowering of the stimulation frequency resulted in a partial (and reversible) reversal of the synaptic fatigue (Fig. 2*A*). In these experiments (8/9 performed in the presence of D-AP5 and LY-341495) the 0.2-Hz stimulation caused a total fatigue of the AMPA EPSC to $44 \pm 4.9\%$ ($n = 9$) of the initial value. Note that this value is based on 10 EPSCs just prior to the frequency switch that, in different experiments, occurred after 50–120 stimuli, and not after 40–60 stimuli as above. After the switch to 0.033 Hz, the AMPA EPSC amplitude decreased to $54 \pm 4.9\%$ ($n = 9$) of the initial value. A further lowering of the frequency from 0.033 to 0.017 Hz did not lead to any further change in the AMPA EPSC ($-1.5 \pm 1.7\%$, $n = 7$), demonstrating that this readily reversible depression only develops at frequencies above 0.033 Hz. We will henceforth refer to this readily reversible component of fatigue, observed when altering the frequency from 0.033 Hz to 0.2 Hz, as low-frequency depression. These results thus suggest that there is a readily reversible low-frequency depression that causes an EPSC reduction by 19% ((54 – 44)/54) and a non-readily reversible component of fatigue that causes an EPSC reduction by 46% (100 – 54) (assuming that these two components are independent of each other, i.e. multiplicatively related). The magnitudes of the low-frequency depression and of the non-readily reversible component of the synaptic fatigue were found not to correlate ($r = 0.20$, $P > 0.05$, $n = 9$).

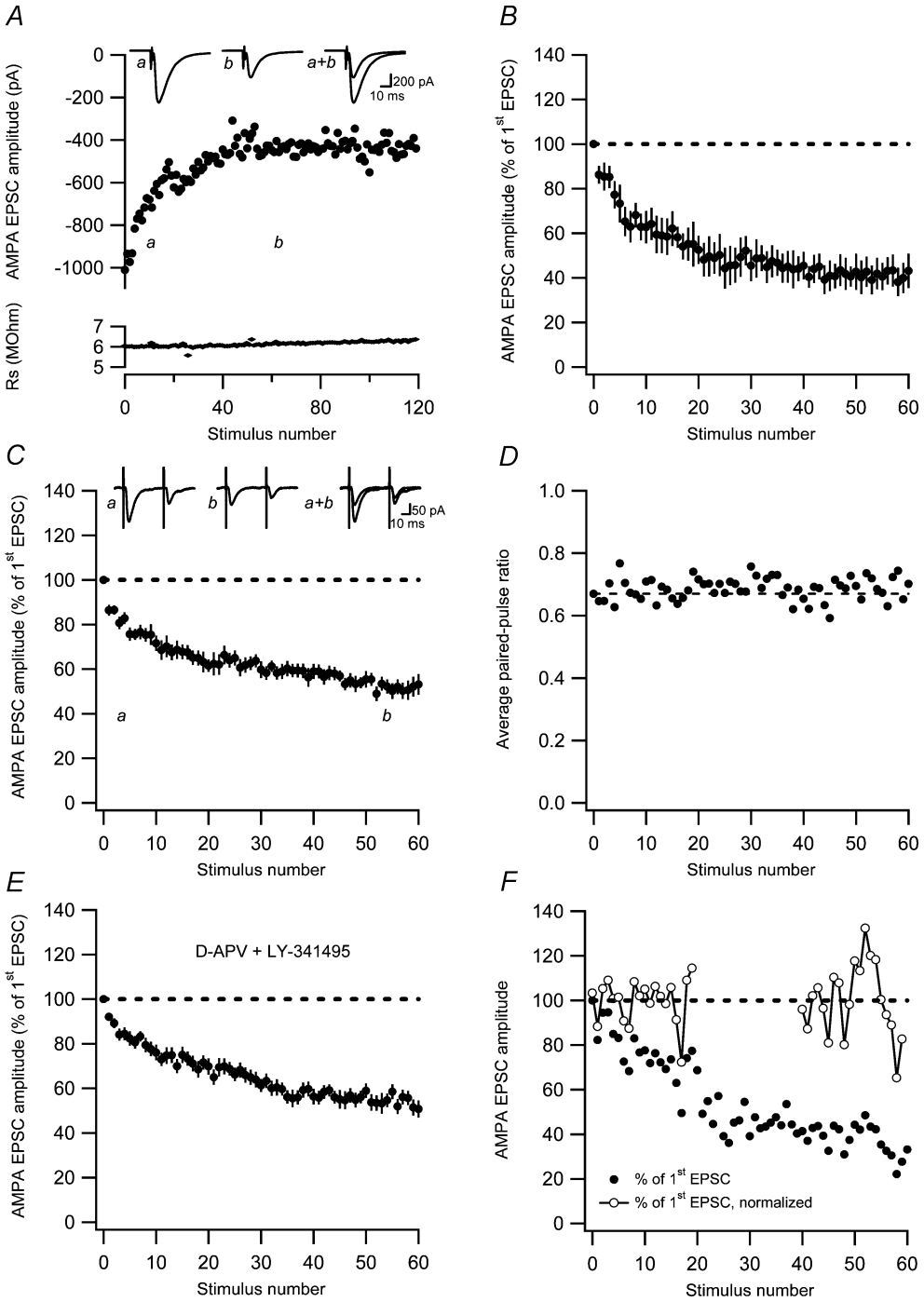


**Figure 1. AMPA EPSC fatigue at previously unstimulated (naive) developing PP–GC synapses**
*A*, an experiment illustrating AMPA EPSC fatigue at 0.2-Hz stimulation at −80 mV. Measurements of series resistance are plotted *versus* stimulus number in the lower graph. Average EPSCs ($n = 10$) taken at time points *a* and *b* are shown as insets. *B*, AMPA EPSC fatigue in response to single stimulation at 0.2 Hz ($n = 7$) as a function of stimulus number. Before averaging, the EPSCs in each experiment were normalized with respect to the very first evoked EPSC. *C*, average AMPA EPSC fatigue in response to paired-pulse stimulation (50 ms) at 0.2 Hz as a function of stimulus number ($n = 10$). Representative average EPSCs ($n = 10$) taken at time points a and b are shown as insets. *D*, average paired-pulse ratio during synaptic fatigue plotted as a function of stimulus number. The paired-pulse ratio measurements were constructed as ratios between average ($n = 10$ experiments) second and first EPSCs. Dashed line indicates the paired-pulse ratio of the first stimulus. *E*, AMPA EPSC fatigue in the presence of the NMDA receptor antagonist D-AP5 (50 $\mu$M) and the mGlu receptor antagonist LY-341495 (20 $\mu$M; $n = 16$). AMPA EPSCs were evoked by single stimulation at 0.2 Hz. *F*, AMPA EPSC variability during synaptic fatigue. An experiment illustrating AMPA EPSC fatigue at 0.2-Hz stimulation at −80 mV. AMPA EPSC amplitudes

To evaluate the pharmacology of the low-frequency depression in isolation, separate experiments were performed in which stable EPSC amplitudes were first obtained at 0.033 Hz before switching to 0.2 Hz (Fig. 2*B*). In the control situation, this frequency switch led to a depression of $27 \pm 2.9\%$ ($n = 8$). To directly compare this value with that obtained above in the presence of D-AP5 (50 $\mu$M) and LY-341495 (20 $\mu$M), we calculated the depression caused by switching back from 0.033 to 0.2 Hz (see Fig. 2*Ab* and *c*). The depression so calculated amounted to $27 \pm 2.3\%$ ($n = 8$) (indicative of a small continuous decrease in baseline), demonstrating that mGlu and NMDA receptor activation are not involved in the generation of the low-frequency depression.

As the switch to 0.033 Hz only removed a lesser component of the fatigue, this very low stimulation frequency, when applied to a naive synaptic input, would be expected to lead to a substantial depression. Figure 2*C* shows that this is indeed the case, the AMPA EPSC amplitude decaying to $70 \pm 10\%$ ($n = 12$) of the naive AMPA EPSC within 15–20 stimuli. This depression agrees well with that observed in Fig. 1 (using 0.2 Hz) after a corresponding number of stimuli (and correction for a fully developed low-frequency depression). This non-readily reversible depression might then be AMPA silencing because this silencing (in CA1 pyramidal neurones) is not readily reversible and is evoked by very low frequencies (Xiao *et al.* 2004).

### AMPA silencing may explain the non-readily reversible component of AMPA EPSC fatigue in the developing rat

If a total silencing of AMPA signalling at a subset of synapses partly explains the fatigue, it should be possible to observe a complete disappearance of AMPA signalling provided that only one or a few susceptible synapses are activated. Using our approach with preset stimulation intensity, naive AMPA EPSCs displaying failures of AMPA signalling (in the beginning of the experiments) were observed in six of the experiments (not included in Fig. 1*C*). In two of these six experiments a complete AMPA silencing was observed, as illustrated from one of these experiments (Fig. 3). It can be seen that there is a mixture of failures and a few successful AMPA EPSCs initially, that the AMPA EPSCs disappear completely despite remaining NMDA EPSCs, and that no AMPA EPSCs are present after switching back from +40 mV to −80 mV.

### Fatigue of NMDA EPSCs at naive synaptic inputs in the developing rat

The synaptic fatigue of naive NMDA EPSCs were examined at +40 mV. The average ($n = 16$) time course of this fatigue, based on results using both single and paired-pulse test stimuli (at 0.2 Hz), is shown in Fig. 4*A* and indicates a substantial NMDA EPSC depression within 40–60 stimuli (to $60 \pm 3.2\%$ of the initial value, $n = 16$), with no difference between using single ($59 \pm 2.5\%$, $n = 5$) or paired-pulse ($60 \pm 4.5\%$, $n = 11$) stimulation.

When raising the stimulation frequency from 0.033 to 0.2 Hz (cf. Fig. 2*B*), the NMDA EPSCs decreased by $27 \pm 2.2\%$ ($n = 6$) (Fig. 4*B*); that is, the same as the AMPA EPSC (see above). Thus, the readily reversible component of the synaptic fatigue involves AMPA and NMDA EPSCs equally. Moreover, this result suggests that there is also a non-readily reversible component contributing to the NMDA EPSC fatigue.

### The non-readily reversible component of synaptic fatigue is not the same for AMPA and NMDA EPSCs

If the non-readily reversible component of AMPA EPSC fatigue is AMPA silencing, then the non-readily reversible component of NMDA EPSC fatigue should be based on a different kind of plasticity process. To test this notion, we examined the interaction between synaptic fatigues elicited at −80 mV and at +40 mV (at 0.2 Hz). In the first set of interaction experiments ($n = 7$), fatigue was first elicited at +40 mV, and the holding potential then switched to −80 mV to record AMPA EPSCs (Fig. 5*A*). These non-naive AMPA EPSCs were stable (Fig. 5*B*), suggesting that most AMPA EPSC fatigue was already elicited by the preceding synaptic activation at +40 mV. In the converse experiments (Fig. 5*C*), the non-naive NMDA EPSCs decayed to $87 \pm 2.9\%$ ($n = 17$) (Fig. 5*D*), compared with 60% for the naive NMDA EPSCs. This result indicates that the preceding synaptic activation at −80 mV had not been sufficient to elicit full fatigue of the NMDA EPSCs, suggesting that a considerable part (see below) of the NMDA EPSC decrease (at +40 mV) is distinct from that of the AMPA EPSC decrease at −80 and at +40 mV.

It may be noted that the NMDA EPSCs observed following the switch from −80 to +40 mV show no tendency for an initial increase, but rather demonstrate a small continuous decay (Fig. 5*D*). Thus we did not observe any evidence for a depolarization-induced increase in presynaptic release probability (Voronin *et al.* 2004).

are normalized with respect to the very first evoked EPSC (●). EPSC amplitudes are also shown normalized with respect to the average EPSC amplitude during the first 20 sweeps and during sweep 40–60 (○–○). Note that the variability increases towards the end of the fatigue protocol.

As shown above, the synaptic fatigue consists of one low-frequency depression component that reduces the EPSC to 73%, irrespective of whether the cell is held at −80 or at +40 mV. As the total fatigue of naive NMDA EPSCs at +40 mV reduces the NMDA EPSC to 60%, the remaining non-readily reversible component should reduce the NMDA EPSC to 82% (60/73). The interaction results above, showing a decay of the non-naive NMDA EPSC to 87%, suggest that most of this remaining component of the NMDA EPSC fatigue (recorded at +40 mV) is only elicited at +40 mV. As a consequence, most of the non-readily reversible component of the AMPA EPSC fatigue (reducing the AMPA EPSC to 70% (51/73) (total AMPA EPSC fatigue was to 51%; see above)) should not be associated with an NMDA EPSC reduction. In other words, this component seems selective for AMPA receptor-mediated transmission and may thus be AMPA silencing. This result is also fully consistent with the depression of the AMPA EPSC to 70% elicited by stimulation at 0.033 Hz (Fig. 2*C*), a frequency that is too low to elicit any reversible low-frequency depression. Note, however, that these estimates of the amount of AMPA silencing are based on measurements taken before the full development of the fatigue process. They are thus underestimated compared with the depression to 54% caused by the AMPA silencing component (see Figure 2*A*), which was based on later measurements.

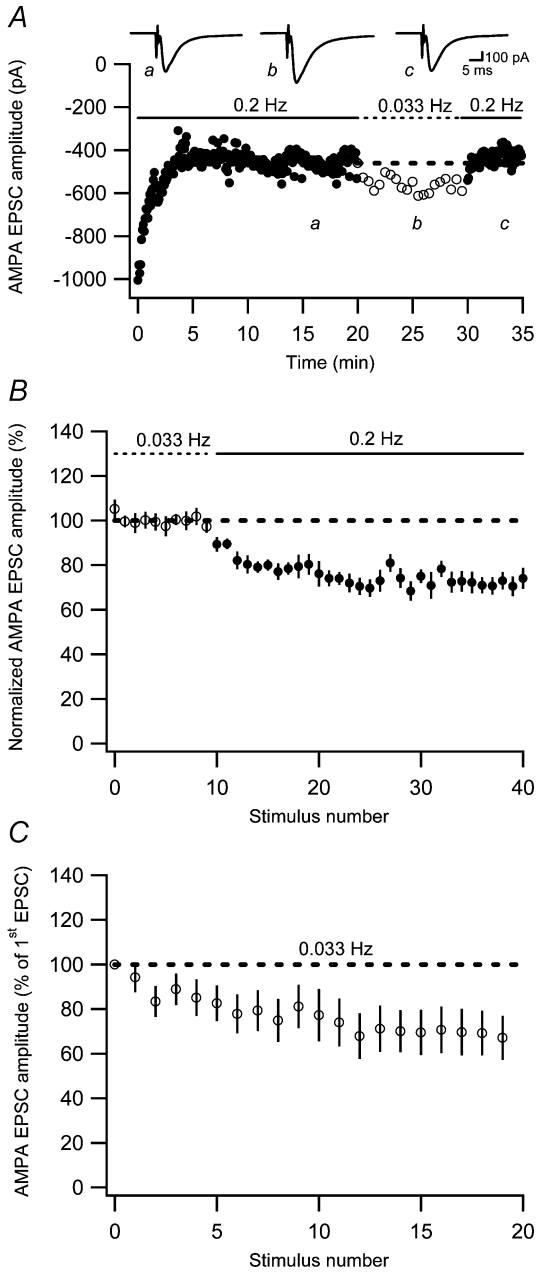


**Figure 2. Two components of AMPA EPSC fatigue**
*A*, an experiment illustrating an initial AMPA EPSC fatigue, followed by a reversible increase in AMPA EPSC amplitude when switching the stimulation frequency from 0.2 to 0.033 Hz. Average EPSCs ($n = 10$) at the different stimulation frequencies are shown as insets. Dashed line represents average AMPA EPSC amplitude just before switching to 0.033 Hz. *B*, graph showing decrease of AMPA EPSC when switching from 0.033 to 0.2 Hz ($n = 8$). *C*, average AMPA EPSC fatigue in response to stimulation at 0.033 Hz as a function of stimulus number ($n = 12$).

## The naive PP–GC synapse in the developing rat signals via both AMPA and NMDA receptors

Developing CA3–CA1 synapses signal via both AMPA and NMDA receptors in their naive state (Groc *et al.* 2002; Xiao *et al.* 2004). If this is also the case for developing PP–GC synapses, one would expect that AMPA silencing creates a different quantal content for AMPA and NMDA EPSCs that corresponds to the number of synapses that undergoes AMPA silencing. As shown above (Fig. 2*A*), after AMPA silencing 54% ± 4.9% ($n = 9$) of the synapses still showed AMPA signalling, predicting that $1/CV^2$ late$_{AMPA}$ at the end of the fatigue period should be 54% of that of the $1/CV^2$ $_{NMDA}$. To test this prediction we calculated $1/CV^2$ for the AMPA EPSCs at the end of the fatigue period and it compared with the $1/CV^2$ value for the subsequently recorded NMDA EPSCs, as indicated in Fig. 6*A* (see also Fig. 5). The $1/CV^2$ late$_{AMPA}$ was 59 ± 11% ($n = 17$) of the $1/CV^2{}_{NMDA}$ (Fig. 6*B*). This comparison indicates that the presence of AMPA silent synapses, as evaluated by a difference in AMPA and NMDA EPSC variability, is created by the low-frequency activation.

## AMPA EPSC fatigue in the adult rat consists only of low-frequency depression

When examined in the adult rat (30–47 days old), the naive AMPA EPSC decreased (at 0.2 Hz) to 75 ± 3.8% of its initial value ($n = 10$) (Fig. 7*A*). This fatigue was significantly smaller ($P < 0.001$) than the fatigue observed in the younger group (7–12 days old). In a subset of these

experiments ($n = 5$), the stimulus rate was changed from 0.2 to 0.033 Hz after the initial fatigue. This lowering of the stimulus rate resulted in an almost complete recovery of the AMPA EPSC fatigue (Fig. 7*B*), indicating that AMPA EPSC fatigue in the adult rat consists of the readily reversible low-frequency depression. The magnitude of the low-frequency depression *per se* in the adult rat was estimated in a separate set of experiments by changing the stimulus rate from 0.033 to 0.2 Hz, and it amounted to $22 \pm 1.9\%$ ($n = 9$). This magnitude of the low-frequency depression accounts well for the total AMPA EPSC fatigue at this age (to 75% of the initial value, see above) and it was not significantly different from that in the younger group ($P > 0.05$). As for the AMPA EPSC, the low-frequency depression of NMDA EPSCs in the adult ($26 \pm 4.1\%$, $n = 5$) was not significantly different ($P > 0.05$) from that in the younger group (27%, Fig. 4*B*). Taken together, these results indicate that there is no developmental trend in the expression of the low-frequency depression.

For the NMDA EPSC, the total fatigue in the adult group was $63 \pm 5.4\%$ ($n = 7$) of the initial value, and was not significantly different ($P > 0.05$) from that observed in the younger group (60%, Fig. 4*A*). As the low-frequency depression did not change with development, this result indicates that the non-readily reversible component of NMDA EPSC fatigue, in contrast to that of the AMPA EPSC fatigue, does not disappear with development.

### Low-frequency depression is not associated with changes in paired-pulse ratio

As shown above (Fig. 1), the AMPA EPSC fatigue is associated with a decrease in $1/CV^2$ and with no change in the paired-pulse ratio. As low-frequency depression constitutes a considerable part of the AMPA EPSC fatigue in the developing rat, it is also likely that the low-frequency depression is associated with a decrease in $1/CV^2$ and with no change in the paired-pulse ratio. We tested this assumption directly and confirmed that the low-frequency depression of the AMPA EPSC ($26 \pm 1.9\%$, $n = 29$, 7- to 47-day-old rats), when altering the frequency from 0.033 to 0.2 Hz, was associated with a decrease in the $1/CV^2$ ($45 \pm 5.4\%$, $n = 29$) and with no significant change in the paired-pulse ratio ($3.4 \pm 4.2\%$, $n = 19$, $P > 0.05$). The reduction in $1/CV^2$, together with the fact that the low-frequency depression is expressed to the same extent by AMPA and NMDA EPSCs (Figs 2 and 4), implies a decrease in the number of active synapses and/or a reduction in presynaptic release probability. A reduction in release probability is thought to be associated with an increase in the paired-pulse ratio (Zucker & Regehr, 2002). However, release probability for the individual synapses is a function of two factors, the number of readily releasable vesicles and the release probability of the individual vesicle (Hanse & Gustafsson, 2001*c*). A reduction of the latter factor, but not the former, is expected to be associated with an increase in paired-pulse ratio (Hanse & Gustafsson, 2001*a*). To examine the average change in paired-pulse ratio in a more unbiased manner, we performed the analysis described above (Fig. 1*D*). Figure 8*A* shows that using this procedure there was also no change in paired-pulse ratio associated with the low-frequency depression.

We also tested whether low-frequency depression was related to paired-pulse plasticity. As shown previously (Harris *et al.* 1979), both portions of the perforant path, the medial and the lateral perforant path, express low-frequency depression. These groups of synapses differ in paired-pulse plasticity, the medial perforant path synapses generally exhibiting paired-pulse depression

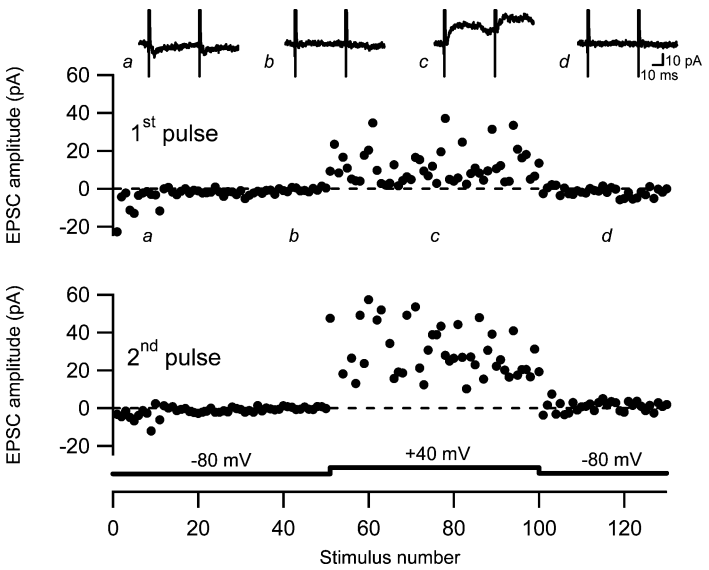


**Figure 3. Silencing of AMPA receptor-mediated signalling**
An experiment illustrating sequential recordings of naive AMPA EPSCs (at −80 mV), NMDA EPSCs (at +40 mV) and AMPA EPSCs (at −80 mV). Paired-pulse stimuli (50 ms) were given at 0.2 Hz. The upper graph shows the amplitude of the first EPSC and the lower graph shows the amplitude of the second EPSC. Amplitudes are plotted *versus* stimulus number. Average EPSCs ($n = 10$) taken at time points indicated by *a*–*d* are shown on top.

whereas the lateral perforant path synapses generally exhibit paired-pulse facilitation (McNaughton, 1980). In these experiments we used extracellular recordings placing the recording and stimulation electrodes at various distances from the granule cell layer (Hanse & Gustafsson, 1992). We found no relationship between the amount of low-frequency depression and the paired-pulse ratio (Fig. 8*B*).

### Low-frequency depression is associated with a decrease in vesicle pool size

The absence of any obvious shift in paired-pulse ratio in association with the low-frequency depression (Fig. 8*A*) suggests that this depression is not caused by any mechanism reducing the release probability of the individual vesicle (Hanse & Gustafsson, 2001*c*). On the other hand, a decrease in release probability related to a decrease in the number of readily releasable vesicles can occur without any change in paired-pulse ratio (see Hanse & Gustafsson, 2001*a*). An estimate of the relative number of readily releasable vesicles can be obtained by analysing the response to brief high-frequency stimulation (Schneggenburger *et al.* 1999; Wasling *et al.* 2004). The idea behind this analysis is that the relative stability of the EPSC magnitude during the later part of the train response is explained by an equilibrium between release and recruitment of vesicles. Practically, the cumulative EPSC responses during the train stimulation are first calculated. Then a linear regression for the later, linear part of the cumulative response is calculated. Finally this line is extrapolated to the first stimulus. The slope of the regression line will represent the recruitment rate of new vesicles and the extrapolation of the regression line to the first stimulus provides an estimate of the number of readily releasable vesicles present at the first stimulus (i.e. the preprimed pool of vesicles; Hanse & Gustafsson, 2001*c*).

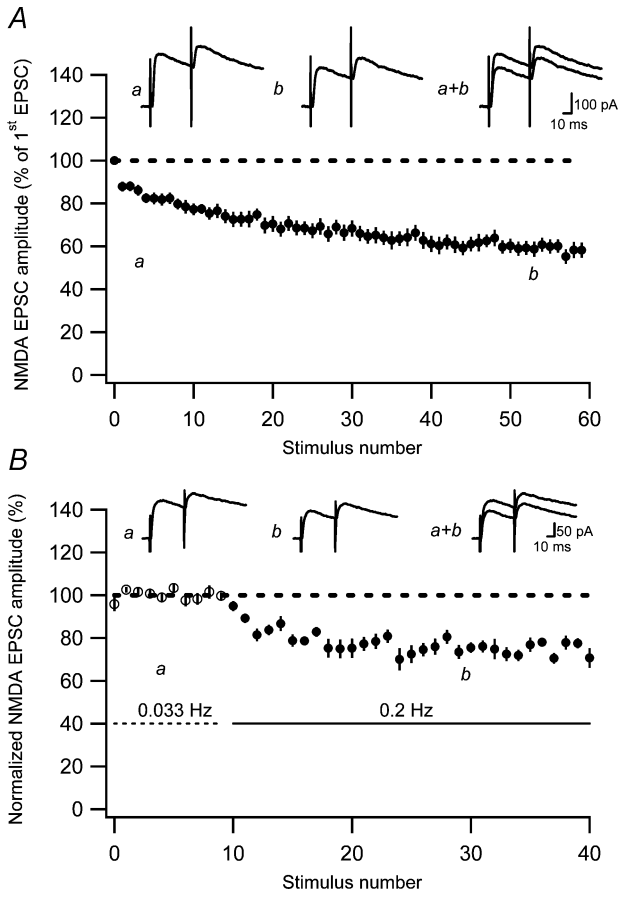


**Figure 4. NMDA EPSC fatigue at previously unstimulated (naive) developing PP–GC synapses**
*A*, average NMDA EPSC fatigue in response to both single and paired-pulse stimulation (50 ms) at 0.2 Hz as a function of stimulus number ($n = 16$). Representative average EPSCs ($n = 10$) taken at the beginning (*a*) and the end (*b*) of the fatigue protocol are shown on top. *B*, low-frequency depression of NMDA EPSCs. Graph shows average ($n = 6$) decrease of NMDA EPSCs when switching from 0.033 to 0.2 Hz. Before averaging, the EPSCs in each experiment were normalized with respect to the average EPSC amplitude evoked at 0.033 Hz. Representative average EPSCs ($n = 10$) taken at time points indicated by *a* and *b* are shown on top.

To estimate the vesicle pool size and its possible changes in association with the low-frequency depression, we performed whole-cell voltage-clamp experiments using train stimulation (10 impulses, 50 Hz), instead of single or paired-pulse stimulation, as the test stimulus. These trains were evoked at 0.2 Hz and at 0.033 Hz. An example of responses to such stimulation is illustrated in Fig. 9*A* (dashed line, 0.033 Hz; continuous line, 0.2 Hz). Figure 9*B* compares the amount of low-frequency depression (of the first EPSC) when single (left), paired-pulse (middle), or train stimulation (right) was used as the test stimulus. Whereas single and paired-pulse stimulation resulted in about the same amount of depression ($25 \pm 2.3\%$; $n = 10$ and $27 \pm 2.6\%$; $n = 19$, respectively), the train stimulation was associated with a considerably larger depression of the first EPSC in the train ($60 \pm 9.9\%$, $n = 7$). This larger depression was not associated with any significant change in paired-pulse ratio ($P > 0.05$) or with any appreciable change in the relative degree of high-frequency depression during the train, as indicated in Fig. 9*C* where the EPSC magnitude (normalized to the first EPSC for each train, and for 0.2-Hz stimulation also scaled to that for 0.033 Hz (dashed line)) is plotted as a function of the stimulus position in the train.

Figure 9*D* shows the cumulative train responses obtained at 0.033 Hz and 0.2 Hz normalized to the first EPSC in the train evoked at 0.033 Hz. The slope of the regression line, and by implication the recruitment rate, was found to be $49 \pm 7.0\%$ ($n = 7$) smaller when the train stimulation was repeated at 0.2 Hz than at 0.033 Hz. The relative magnitude of the estimate of the preprimed pool will depend on when during the train stimulation

recruitment is assumed to start. Assuming full recruitment rate already following the first stimulus in the train, the preprimed pool of vesicles can be estimated by the value of the extrapolated regression line at the first stimulus. This representation of the preprimed pool was $60 \pm 7.4\%$ ($n = 7$) smaller when the train stimulation was repeated at 0.2 Hz than at 0.033 Hz (0.6 *versus* 1.6; expressed in units of the first EPSC in the train evoked at 0.033 Hz). If, on the other hand, recruitment starts abruptly at full rate first when the preprimed pool is depleted, the corresponding values will be 1.2 *versus* 2.7 (also here about 60% reduction). These two estimates of the preprimed pool are based on extreme assumptions and a more reasonable estimate is between these two extremes (that is, 0.9 *versus* 2.15). These latter moderate estimates assume that recruitment starts gradually as the preprimed pool is being depleted (see Hanse & Gustafsson, 2001*c*). Irrespective of the absolute values, this analysis indicates that 5 s between the train stimulations only allows for partial recovery of vesicles both for prepriming and for recruitment during the train stimulation.

## Discussion

The results of the present study demonstrate that naive PP–GC synapses exhibit a pronounced synaptic fatigue. In the developing rat, a stimulus rate of 0.2 Hz leads to a 50% reduction of AMPA-mediated signalling within 50 stimuli. Two separate forms of synaptic plasticity were found to contribute to this synaptic fatigue; a reversible low-frequency depression of presynaptic release probability and a non-readily reversible depression given by AMPA silencing. Our results further indicate that AMPA silencing disappears with maturation whereas the low-frequency depression remains unaltered.

### Low-frequency depression

The low-frequency depression of AMPA transmission was associated with a decrease in quantal content ($1/CV^2$) and with an equal depression of NMDA transmission, indicating a reduction in the number of active synapses, or a depression in release probability. A short-term depression of release probability produced largely at frequencies above 1 Hz, but also to some extent (~10%) at 0.2 Hz, has been described in the Calyx of Held (von Gersdorff *et al.* 1997). This depression has been linked to a reduced calcium influx mediated via calcium-induced inactivation of voltage-gated calcium channels (Xu & Wu, 2005). Such a mechanism would be expected to result in increases in the paired-pulse ratio (Zucker & Regehr,

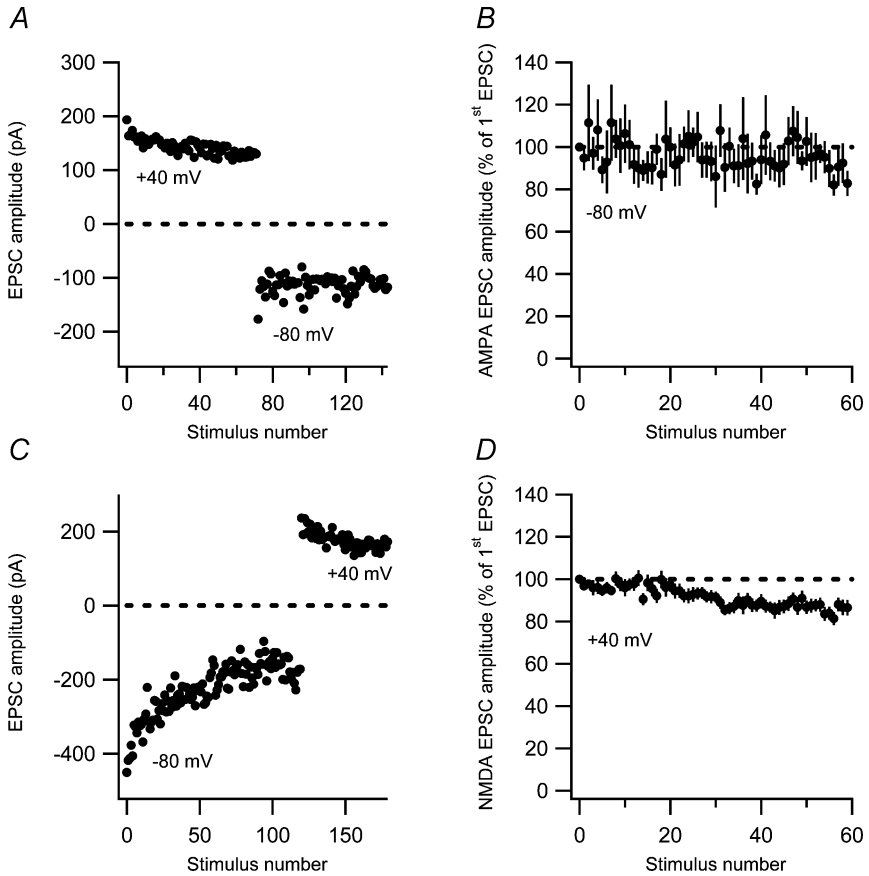


**Figure 5. Interaction between synaptic fatigue induced at −80 and +40 mV**
*A*, an experiment illustrating sequential recordings of naive NMDA EPSCs (at +40 mV) and AMPA EPSCs (at −80 mV). Note the difference in variability between NMDA ($1/CV^2 = 213$) and AMPA ($1/CV^2 = 43$) EPSCs. *B*, AMPA EPSCs evoked after the preceding fatigue protocol at +40 mV. AMPA EPSC amplitude is plotted *versus* stimulus number ($n = 7$). *C*, an experiment illustrating sequential recordings of naive AMPA EPSCs (at −80 mV) and NMDA EPSCs (at +40 mV). Note the difference in variability between NMDA ($1/CV^2 = 200$) and AMPA ($1/CV^2 = 61$) EPSCs. *D*, NMDA EPSCs evoked after the preceding fatigue protocol at −80 mV. NMDA EPSC amplitude is plotted *versus* stimulus number ($n = 17$).

2002), which, however, were not observed in this study. Thus, a reduction in release probability involving reduced calcium influx does not seem to be responsible for the low-frequency depression. Instead, we consider two other possible mechanistic scenarios that would account for the present findings; a reversible and total presynaptic silencing at a subset of the synapses, and a reduction in release probability that is not associated with an increased paired-pulse ratio.

With respect to the first scenario, in *Aplysia* there is a short-term habituation of the gill withdrawal reflex that is caused by homosynaptic depression at the sensorimotor neurone synapses and for which a total silencing of a subset of synapses has been proposed as the most likely mechanism (Gover *et al.* 2002). The low-frequency depression at the PP–GC synapse has previously been termed habituation (Teyler & Alger, 1976), and it also exhibits features in common with behavioural habituation (Christoffersen, 1997). Both the present low-frequency depression and the homosynaptic depression in *Aplysia* (Castellucci & Kandel, 1974; Gover *et al.* 2002) are induced by a few stimuli at low frequency and expressed as a reduction in quantal content with no consistent change in paired-pulse ratio. However, the homosynaptic depression in *Aplysia* can be induced by interstimulus intervals up to 5 min and it recovers over tens of minutes (see Gover *et al.* 2002), properties which clearly distinguishes it from the presently described low-frequency depression that is not evoked at 0.033 Hz and recovers in seconds. It is, however, interesting that these temporal features of the homosynaptic depression in *Aplysia* (as well as a reduction in quantal content with no consistent change in paired-pulse ratio) agree very well with those of AMPA silencing (present study; Xiao *et al.* 2004). In fact, recent experiments on the CA3–CA1 synapses have shown that AMPA silencing spontaneously reverses within tens of minutes (authors' unpublished observations).

With respect to the second scenario, a change in release probability can occur without changes in the paired-pulse ratio (Honda *et al.* 2000) if it is caused by a reduced probability of having vesicles ready to be released (primed) just prior to the moment of stimulation, i.e. by a reduced preprimed pool of vesicles (Hanse & Gustafsson, 2001*a*). Such a reduction will not increase the paired-pulse ratio because the second of the paired responses will be as affected by the reduction in preprimed pool as the first response. A stimulus-dependent reduction of the preprimed vesicle pool may easiest be explained if vesicles are released at a higher rate than that at which they are replenished, a phenomenon referred to as depletion. Although direct evidence is often lacking, depletion is generally thought of as the main mechanism underlying short-term depression (Thomson, 2000). Because tests for depletion have commonly been performed using high levels of stimulation, it is unclear to what extent depletion should occur in response to single action potentials evoked

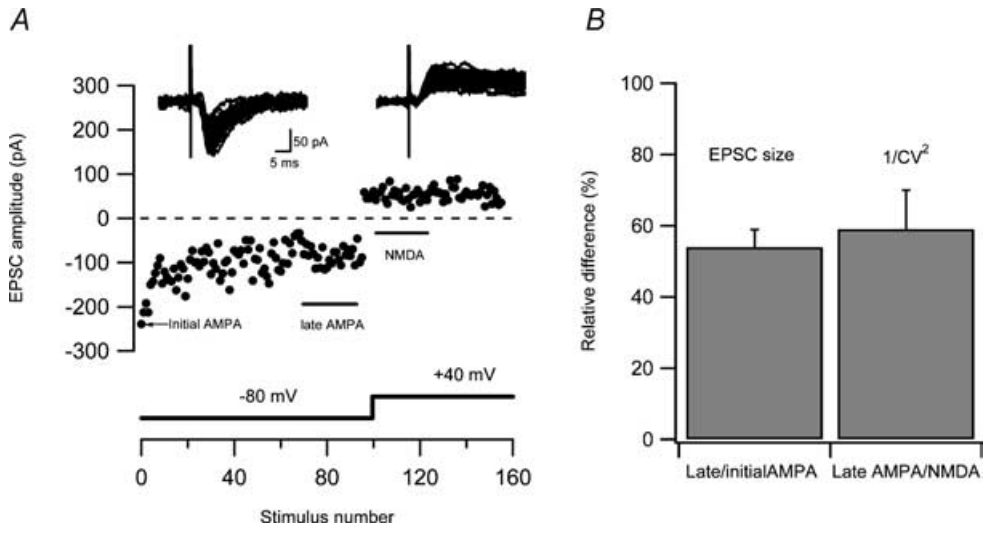


**Figure 6. Comparison of $1/CV^2$ for AMPA and NMDA EPSC**
*A*, an experiment illustrating sequential recordings of naive AMPA EPSCs (at −80 mV) and NMDA EPSCs (at +40 mV). Data points for calculation of $1/CV^2$ for late AMPA and NMDA EPSCs were taken at time intervals indicated in the graph. The EPSCs evoked during these time intervals are shown as insets above. In this experiment the $1/CV^2$ for late AMPA and NMDA EPSCs were 11 and 16, respectively. *B*, bar graph comparing difference in $1/CV^2$ between AMPA and NMDA EPSCs with AMPA silencing. Left bar shows the percentage of AMPA signalling synapses left after AMPA silencing. These values were taken from experiments ($n = 9$) such as that illustrated in Fig. 2*A*, in which the AMPA silencing component was obtained in isolation from the low-frequency depression. Right bar shows the relative percentage of $1/CV^2_{\text{lateAMPA}}$ to $1/CV^2_{\text{NMDA}}$ from experiments ($n = 17$) such as that illustrated in *A*.

at 5-s intervals. Using experimental depletion protocols, for example long high-frequency trains of presynaptic activation or hypertonic shocks, it has been found that hippocampal synapses recover from depletion with a time constant of about 5–10 s (see Stevens & Wesseling, 1998). If such time constants were applicable also for the depletion induced by single action potentials, and if the preprimed pool of vesicles at PP–GC synapses is small, depletion may account for the presently observed low-frequency depression. In the present study we estimated the size of the preprimed pool of vesicles (relative to the release causing the first EPSC) based on the cumulative release during 10-impulse 50-Hz trains (Fig. 9*D*). The size of the preprimed pool can be expressed in units of release probability (of the first EPSC) given that quantal size, and the number of activated synapses, is not altered during the train (Hanse & Gustafsson, 2001*b*). Using a moderate estimate (see Results), we found that the preprimed pool was 2.15 times the release probability. Even if the average release probability should be as large as 0.5 (at 0.033 Hz), the preprimed pool size at the PP–GC synapse would thus not be much larger than one vesicle (i.e. about that estimated for the CA3–CA1 synapse; Hanse & Gustafsson, 2001*c*), consistent with a high sensitivity to depletion.

The analysis of the release during the 10-impulse 50-Hz trains evoked at 0.033 and 0.2 Hz, indicated a 2.5-fold smaller size of the preprimed pool at the higher frequency. This result is consistent with depletion being responsible for the low-frequency depression, at least following train stimulation. As both train and paired-pulse stimulation resulted in low-frequency depression that did not interact with short-term plasticity, it may be assumed that paired-pulse and train stimulations, as well as single volley stimulation, elicit the same low-frequency depression, but to different extents. Based on the cumulative EPSC amplitude during the 10-impulse train, it can be estimated that single stimuli would release 22%, and paired-pulse stimuli would release 35%, of the amount released by

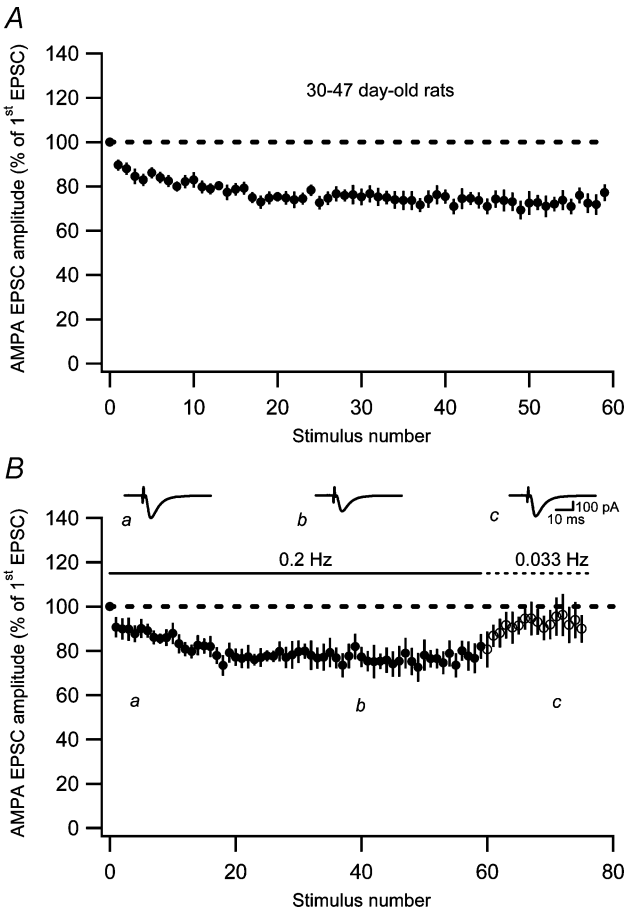


**Figure 7. Synaptic fatigue in adult PP–GC synapses**
*A*, AMPA EPSC fatigue evoked at 0.2 Hz at previously unstimulated (naive) adult (30- to 47-day-old rats) PP–GC synapses ($n = 10$). *B*, AMPA EPSC fatigue evoked at 0.2 Hz followed by recovery after switching to 0.033 Hz ($n = 5$). Representative average EPSCs ($n = 10$) taken at time points indicated by *a*–*c* are shown as insets.

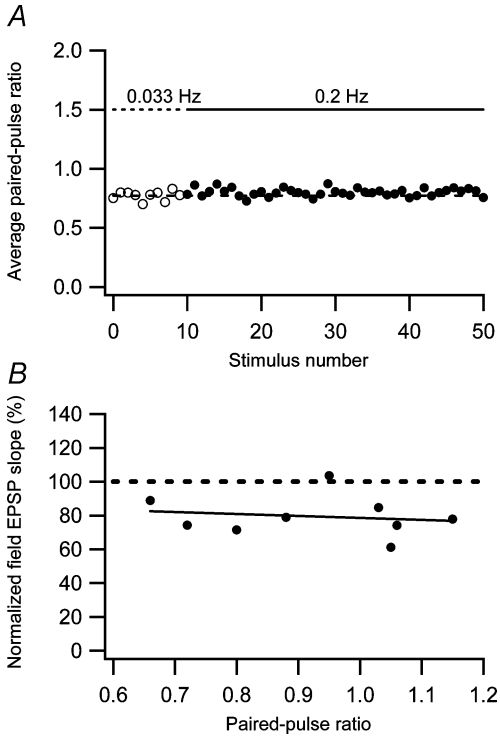


**Figure 8. Relationship between low-frequency depression and paired-pulse plasticity**
*A*, there is no change in paired-pulse ratio in association with low-frequency depression. Average paired-pulse ratio during low-frequency depression is plotted as a function of stimulus number. The paired-pulse ratio measurements were constructed as ratios between average ($n = 19$ experiments) second and first EPSCs. The dashed line is an average of the first 10 measurements evoked at 0.033 Hz. *B*, low-frequency depression is not correlated with paired-pulse plasticity. The amount of low-frequency depression measured using field EPSPs is plotted against the paired-pulse ratio ($n = 9$). The dashed line represents a linear regression through the data points ($r = -0.16$, $P > 0.05$).

all the 10 stimuli in the train. These values could be translated to 13% (22% of the 60% depression produced by train stimulation) and 21% low-frequency depression following single and paired-pulse stimuli, respectively. Whereas this estimation agrees well for paired-pulse stimuli (27% depression observed), there is a considerable discrepancy with respect to single stimuli (25% depression observed). It may be that various degrees of recruitment play a role here. Thus, calcium influx following single stimuli at a low rate may be proportionally less efficient in initiating vesicle recruitment than that following multiple presynaptic action potentials at a high rate (see Moulder & Mennerick, 2005).

The results of the present study show that the low-frequency depression is already established in the early period of synaptogenesis (7- to 12-day-old rats) and remains unaltered into adulthood, and that it is expressed to about the same extent in parts of the perforant path exhibiting different paired-pulse plasticity (depression and facilitation). The low-frequency depression, which may be functionally important as a filter favouring novel synaptic activity from the entorhinal cortex to the hippocampus, appears thus to be a robust hallmark of the PP–GC synapse.

### Activity-dependent creation of AMPA-silent synapses

Our results suggest that part of the synaptic fatigue in the developing, but not in the adult, rat is explained by AMPA silencing. This conclusion is based on five different

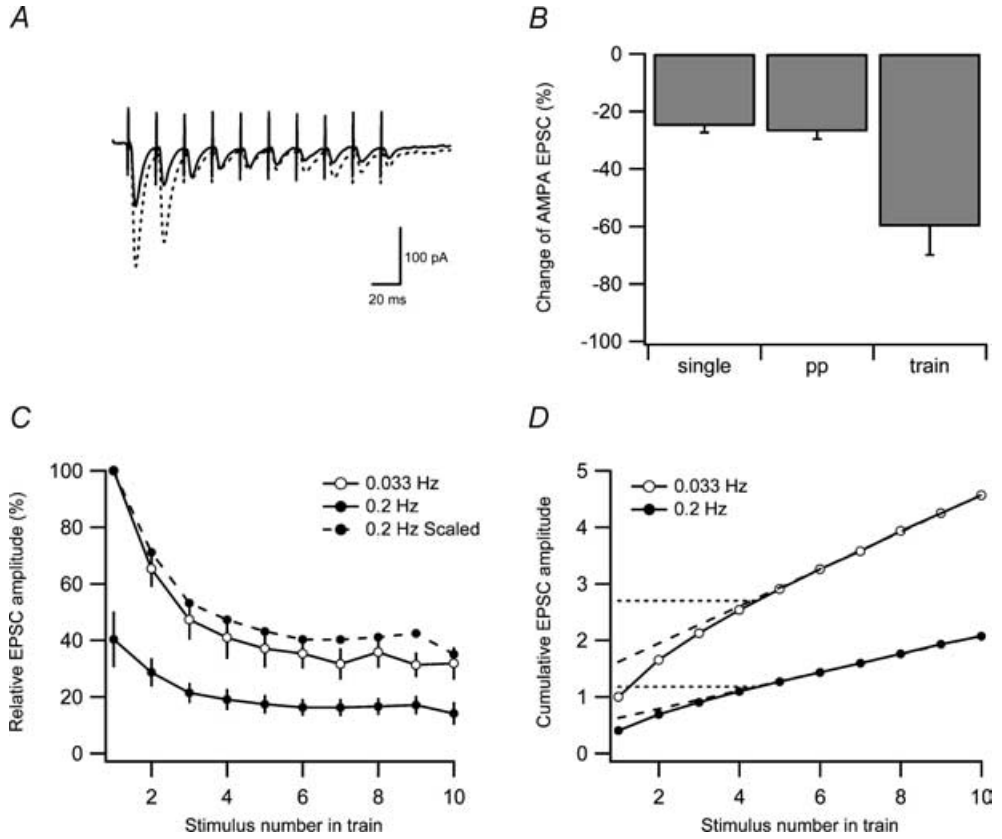


**Figure 9. Estimation of vesicle pool size during low-frequency depression**
*A*, examples of average ($n = 10$) responses to 10-impulse 50-Hz stimulation trains evoked at 0.033 Hz (dashed line) and at 0.2 Hz (continuous line). *B*, bar graph showing the average change of the AMPA EPSC when using single ($n = 10$), paired-pulse (PP) ($n = 19$) and train ($n = 7$) stimulation. *C*, average AMPA EPSC amplitudes in response to 10-impulse 50-Hz stimulation trains evoked at 0.033 Hz (○) and at 0.2 Hz (●). AMPA EPSC amplitudes are plotted *versus* stimulus number in the 50-Hz train and they were normalized to the first EPSC in the train evoked at 0.033 Hz before averaging. Filled circles connected by dashed line is the same as filled circles connected with continuous line, but scaled such that the first EPSC amplitude in the train is 100%. *D*, cumulative AMPA EPSC amplitude during 50-Hz train stimulation based on the EPSC amplitudes in *C*. Dashed lines are extrapolations from linear regression over the last five data points. Intersection between dashed line and the *y*-axis represents a lower-limit estimation of the pool size. Dotted lines are the horizontal extrapolation from the point where the linear regression line and the cumulative amplitude curve deviate. Intersection between dotted line and the *y*-axis represents an upper-limit estimation of the pool size.

findings: (i) a discrepancy between fatigue of naive AMPA and naive NMDA EPSCs; (ii) a developmental decrease of AMPA EPSC fatigue; (iii) a direct demonstration of AMPA silencing; (iv) a discrepancy in the quantal content ($1/CV^2$) for AMPA and NMDA EPSCs following AMPA EPSC fatigue corresponding to the estimated AMPA silencing; and (v) an insensitivity to pharmacological blockade of mGlu and NMDA receptors.

AMPA silencing evoked by low-frequency stimulation (0.05–0.2 Hz), not requiring NMDA or mGlu receptor activation, has previously been found among developing CA3–CA1 synapses (Xiao *et al.* 2004). At those synapses, naive AMPA EPSCs exhibited a substantial fatigue whereas there was little, or no, fatigue of naive NMDA EPSCs recorded at +40 mV. Similar findings have recently been obtained from stratum radiatum interneurones (I. Riebe, B. Gustafsson and E. Hanse, unpublished observations). In contrast, in the present study naive NMDA EPSCs recorded at +40 mV also exhibited a substantial non-readily reversible component of fatigue. However, our interaction experiments (Fig. 5) indicate that, whereas the non-readily reversible component of fatigue affecting AMPA EPSCs was induced to the same extent at both −80 and +40 mV, the fatigue affecting NMDA EPSCs was induced only at +40 mV. As the postsynaptic calcium concentration is expected to be larger at +40 mV, this NMDA EPSC depression might be explained by calcium-dependent inactivation (Rosenmund & Westbrook, 1993); however, we did not explore this possibility further. Irrespective of its mechanism, the present results indicate that the NMDA EPSC depression is not induced by synaptic activation when the cell is voltage clamped at −80 mV. Consequently, the non-readily reversible component of the AMPA EPSC fatigue at −80 mV seems to be selective for AMPA receptor-mediated transmission, consistent with AMPA silencing.

A further dissociation between the non-readily reversible component of AMPA and NMDA EPSC fatigue was their differential developmental profiles. Thus, AMPA EPSC fatigue in the older animals (30–47 days old) was fully reversible when changing to 0.033 Hz, whereas the NMDA EPSC fatigue in these animals was only partially reversible, as in the younger group. These findings suggest that the NMDA EPSC depression induced at +40 mV does not decrease with development whereas AMPA silencing is restricted to the first postnatal weeks. Such developmental restriction for AMPA silencing is fully consistent with previous results from CA3–CA1 synapses (Xiao *et al.* 2004). It also demonstrates that ongoing neurogenesis (and synaptogenesis) in the dentate gyrus of the adult rat is not of sufficient magnitude to impart a significant overall character of 'developmental' plasticity in this structure.

In common with previous findings from developing CA3–CA1 synapses (Xiao *et al.* 2004), the present results suggest that AMPA-silent synapses on dentate granule cells are created by activity and consequently that AMPA silence does not represent the nascent state of glutamatergic synapses. Thus, at the end of synaptic fatigue the $1/CV^2$ value for AMPA EPSCs was about 40% smaller than that for NMDA EPSCs, indicating that the AMPA EPSC was by then mediated by 40% fewer synapses than the NMDA EPSC. Several findings suggest that this mismatch in quantal content between AMPA and NMDA EPSCs was created by the evoked stimulation. First, as discussed above, the non-readily reversible component of synaptic fatigue at −80 mV was selective for the AMPA EPSCs and was associated with a proportional decrease in $1/CV^2$. Second, in two experiments we directly observed the disappearance of AMPA-mediated signalling (Fig. 3). Third, the mismatch in quantal content between AMPA and NMDA EPSCs corresponded well with the estimated decrease in both amplitude and $1/CV^2$ for the AMPA EPSCs during the fatigue (Fig. 6).

### What is naive synaptic strength?

We have used the term 'naive synapses' for synapses that have not been subject to any evoked activity in the slice. One important conclusion from the present study is that naive synaptic strength is clearly different from what is generally referred to as baseline synaptic strength. The existence of synaptic fatigue has implications for the evaluation of other forms of synaptic plasticity and of modulation of synaptic transmission. This is because when experimentally examining plasticity or modulation of synaptic transmission it is normally necessary to first establish a stable baseline of synaptic strength as the control. As the presently described synaptic fatigue is induced even by very modest synaptic activity, it is unavoidably induced while a stable baseline of synaptic strength is established. Thus, a steady-state level of synaptic fatigue is normally the baseline for other forms of synaptic plasticity or synaptic modulation.

## References

Altman J & Das GD (1965). Post-natal origin of microneurones in the rat brain. *Nature* **207**, 953–956.

Castellucci VF & Kandel ER (1974). A quantal analysis of the synaptic depression underlying habituation of the gill-withdrawal reflex in Aplysia. *Proc Natl Acad Sci U S A* **71**, 5004–5008.

Christoffersen GR (1997). Habituation: events in the history of its characterization and linkage to synaptic depression. A new proposed kinetic criterion for its identification. *Prog Neurobiol* **53**, 45–66.

Clements JD (1990). A statistical test for demonstrating a presynaptic site of action for a modulator of synaptic amplitude. *J Neurosci Methods* **31**, 75–88.

Gover TD, Jiang XY & Abrams TW (2002). Persistent, exocytosis-independent silencing of release sites underlies homosynaptic depression at sensory synapses in Aplysia. *J Neurosci* **22**, 1942–1955.

Groc L, Gustafsson B & Hanse E (2002). Spontaneous unitary synaptic activity in CA1 pyramidal neurons during early postnatal development: constant contribution of AMPA and NMDA receptors. *J Neurosci* **22**, 5552–5562.

Hanse E & Gustafsson B (1992). Long-term potentiation and field EPSPs in the lateral and medial perforant paths in the dentate gyrus in vitro: a comparison. *Eur J Neurosci* **4**, 1191–1201.

Hanse E & Gustafsson B (2001*a*). Paired-pulse plasticity at the single release site level: an experimental and computational study. *J Neurosci* **21**, 8362–8369.

Hanse E & Gustafsson B (2001*b*). Quantal variability at glutamatergic synapses in area CA1 of the rat neonatal hippocampus. *J Physiol* **531**, 467–480.

Hanse E & Gustafsson B (2001*c*). Vesicle release probability and pre-primed pool at glutamatergic synapses in area CA1 of the rat neonatal hippocampus. *J Physiol* **531**, 481–493.

Harris EW, Lasher SS & Steward O (1979). Analysis of the habituation-like changes in transmission in the temporodentate pathway of the rat. *Brain Res* **162**, 21–32.

Honda I, Kamiya H & Yawo H (2000). Re-evaluation of phorbol ester-induced potentiation of transmitter release from mossy fibre terminals of the mouse hippocampus. *J Physiol* **529**, 763–776.

Kim J & Alger BE (2001). Random response fluctuations lead to spurious paired-pulse facilitation. *J Neurosci* **21**, 9608–9618.

Korn H & Faber DS (1991). Quantal analysis and synaptic efficacy in the CNS. *Trends Neurosci* **14**, 439–445.

McNaughton BL (1980). Evidence for two physiologically distinct perforant pathways to the fascia dentata. *Brain Res* **199**, 1–19.

Moulder KL & Mennerick S (2005). Reluctant vesicles contribute to the total readily releasable pool in glutamatergic hippocampal neurons. *J Neurosci* **25**, 3842–3850.

Rosenmund C & Westbrook GL (1993). Calcium-induced actin depolymerization reduces NMDA channel activity. *Neuron* **10**, 805–814.

Schlessinger AR, Cowan WM & Gottlieb DI (1975). An autoradiographic study of the time of origin and the pattern of granule cell migration in the dentate gyrus of the rat. *J Comp Neurol* **159**, 149–175.

Schneggenburger R, Meyer AC & Neher E (1999). Released fraction and total size of a pool of immediately available transmitter quanta at a calyx synapse. *Neuron* **23**, 399–409.

Stevens CF & Wesseling JF (1998). Activity-dependent modulation of the rate at which synaptic vesicles become available to undergo exocytosis. *Neuron* **21**, 415–424.

Teyler TJ & Alger BE (1976). Monosynaptic habituation in the vertebrate forebrain: the dentate gyrus examined in vitro. *Brain Res* **115**, 413–425.

Thomson AM (2000). Facilitation, augmentation and potentiation at central synapses. *Trends Neurosci* **23**, 305–312.

von Gersdorff H, Schneggenburger R, Weis S & Neher E (1997). Presynaptic depression at a calyx synapse: the small contribution of metabotropic glutamate receptors. *J Neurosci* **17**, 8137–8146.

Voronin LL, Altinbaev RS, Bayazitov IT, Gasparini S, Kasyanov AV, Saviane C, Savtchenko L & Cherubini E (2004). Postsynaptic depolarisation enhances transmitter release and causes the appearance of responses at 'silent' synapses in rat hippocampus. *Neuroscience* **126**, 45–59.

Wasling P, Hanse E & Gustafsson B (2004). Developmental changes in release properties of the CA3-CA1 glutamate synapse in rat hippocampus. *J Neurophysiol* **92**, 2714–2724.

White WF, Nadler JV & Cotman CW (1979). Analysis of short-term plasticity at the perforant path-granule cell synapse. *Brain Res* **178**, 41–53.

Xiao MY, Wasling P, Hanse E & Gustafsson B (2004). Creation of AMPA-silent synapses in the neonatal hippocampus. *Nat Neurosci* **7**, 236–243.

Xu J & Wu LG (2005). The decrease in the presynaptic calcium current is a major cause of short-term depression at a Calyx-type synapse. *Neuron* **46**, 633–645.

Zucker RS & Regehr WG (2002). Short-term synaptic plasticity. *Annu Rev Physiol* **64**, 355–405.

## Acknowledgements

This project was supported by the Swedish Research Council (project number 01580 and 12600), Åke Wiberg's Foundation, Magnus Bergvall's Foundation and Swedish Society of Medicine. We thank Pontus Wasling for help with software programming.